J Polym Environ (2017) 25:465–478
DOI 10.1007/s10924-016-0806-3

ORIGINAL PAPER

Tailor-Made Electrospun Nanofibers of Biowaste Lignin/Recycled Poly(Ethylene Terephthalate)

Efstratios Svinterikos[1] · **Ioannis Zuburtikudis**[1]

Published online: 30 August 2016

Abstract Producing nanofibers of a desired predetermined diameter is important for all applications where the nano-sized dimension plays a key role. In this research, nanofibers from a blend of lignin and recycled poly(ethylene terephthalate) (PET) were prepared using the electrospinning process. The design of experiments (DoE) statistical methodology was employed to screen the significant factors and optimize the whole process. A fractional factorial design with five electrospinning variables (spinning distance, solution concentration, voltage, lignin ratio and flow rate) was implemented to identify their effect on the average fiber diameter and on its standard deviation. The morphology of the electrospun mats was examined using Scanning Electron Microscopy. The statistical analysis of the measurements revealed that only the spinning distance and the concentration of the spinning solution have significant effect on the two responses. To minimize the average fiber diameter, the method of steepest descent was applied in two distinct experimental areas. After lowering the solution concentration and the spinning distance up to the point of bead formation, the average fiber diameter was minimized to 191 ± 60 nm. Following the method reported here, tailor-made lignin/recycled PET nanofibers of a set, desired diameter can be fabricated by properly adjusting the electrospinning variables.

Keywords Lignin · Poly(ethylene terephthalate) · Nanofibers · Electrospinning · Design of experiments · Optimization

Introduction

The utilization of bio-renewable raw materials in diverse applications is increasingly becoming a subject of extensive research due to the gradual exhaustion of fossil-based resources and the escalation of environmental concerns [1–5]. In the same context, the development of alternative applications for common recycled plastics is of high importance.

One of the most promising bio-renewable raw materials is lignin. It is the second most abundant natural polymer behind cellulose [6] representing around 25–30 % of the total non-fossil organic molecules on earth [1, 2] and being the primary natural source of aromatic compounds [6, 7]. The structure of lignin consists of phenylpropane units (monolignols), but their complex configuration depends on the plant source and its isolation process [4].

Lignin is obtained as a major by-product of the paper industry [6]; it has been estimated that almost 50 million tons are generated every year [1, 2]. Its primary use is as fuel for energy recovery in the industry, a great proportion is discarded as waste [2, 7], and only 2 % of its total annual production is commercially utilized for the manufacture of various products, mainly adhesives and dispersants [2, 8]. However, its potential utilization in various applications such as carbon fiber precursors, polymeric foams and membranes, thermoplastic elastomers or as a component for various polymer composites has been proposed [1, 7]. Lignin possesses several advantageous properties such as high carbon content, compatibility with a variety of

Ioannis Zuburtikudis: Currently on a leave of absence from the Department of Mechanical and Industrial Design Engineering, TEI of Western Macedonia, 50100 Kozani, Greece.

✉ Ioannis Zuburtikudis
izub@teikoz.gr; ioanzub@gmail.com

[1] Department of Chemical and Petroleum Engineering, United Arab Emirates University (UAEU), P.O. Box 15551, Al Ain, United Arab Emirates

chemicals, good thermal stability, adequate reactive functional groups, low cost and biodegradability [1, 2]. However, some limitations such as the heterogeneity of its structure, relatively poor mechanical properties and difficulties in processing still hinder its more widespread use [3].

The total global consumption of plastics increases annually by 5–6 % [9], while poly(ethylene terephthalate) is one of the most widely used commodity plastics and the main material for the manufacture of water bottles [10]. Moreover, PET is the most widely recycled plastic in the USA in terms of weight of plastic material recycled [10]. Therefore, it would be desirable to investigate new potential applications for recycled PET.

Electrospinning is a well-established, versatile technique for the fabrication of submicron polymeric fibers. A schematic setup of the process is presented in Fig. 1. More details on the technique can be found elsewhere [11]. In electrospinning, it is feasible to control the diameter range of the produced fibers by easily adjusting the process and material variables. Reducing the diameter of polymer fibers in the nano-scale enhances their applicability for various industrial, electronic and medical applications [5].

Specifically, nanofibers derived from PET, either alone or in conjunction with other materials, have been proposed for diverse applications including separators, phase change materials for solar and thermal energy storage, substrates for the growth of nanoparticles, membranes and biomedical applications [12–17]. Furthermore, fibers of lignin, especially in conjunction with other polymers, have been proposed as potential carbon fiber precursors [4]. Other potential applications include adsorbents or filters [4]. In all these applications, the surface area plays a decisive role [4, 17]. It is therefore of high importance to control the nano-sized dimension and manufacture nanofibers of desired predetermined diameters. Here it should be stated, that the rigorous definition of nanofibers, demands that the fibers have diameters lower than 100 nm. However, it is very common that the term "nanofibers" is used in the literature for fibers with diameters as large as a few hundreds of nanometers (200–500 nm) [18].

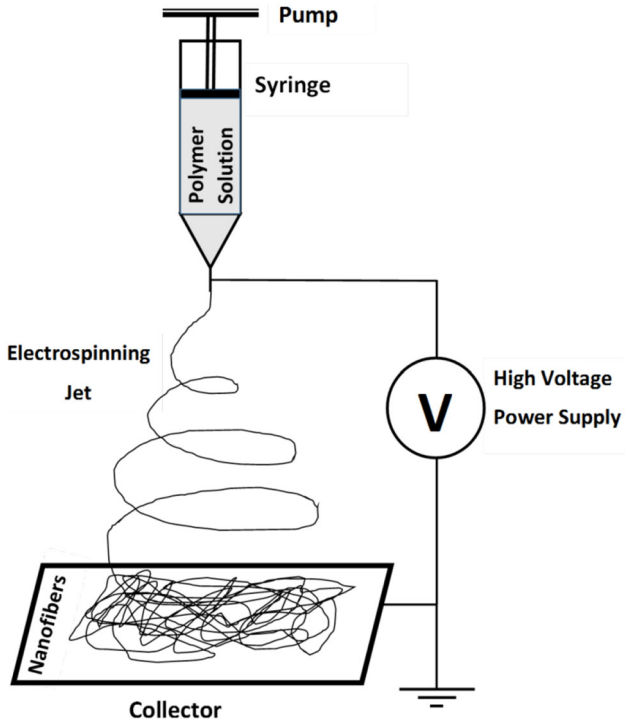

Fig. 1 Schematic electrospinning setup

Fibers of lignin/PET fabricated via melt spinning have been studied before as potential carbon fiber precursors [19–21]. It seems that in such a blend, the weak intermolecular interactions prevail over hydrogen bonding [22]. Fiber diameters in the range of 11–45 μm have been reported [20–22]. Moreover, thermoplastic composites of PET reinforced with lignin using mechanical mixing and thermal extrusion have been reported before [23, 24]. In this case, the composites exhibited good dispersion of lignin particles, enhanced thermal stability and increased PET crystallinity.

Several studies have shown, that various types of lignin cannot be electrospun successfully without being combined with other polymers; only electrospray is formed from lignin alone [25, 26]. This depends on the type of lignin used, since the structure of a specific batch of lignin depends on the source from which the lignin was extracted, the method of extraction and possible treatment [4]. This behavior has been attributed to the relatively low molecular weight of lignin used [25], which influences the solution viscosity, and doesn't prevent the electrospinning jet from breaking easily into droplets before falling on the collector [11]. Hence, the presence of a binder polymer in these cases is necessary for the formation of fibers.

The basis of the research presented here is to combine an inexpensive by-product of the paper industry (lignin) with a widely-used but recycled polymer (PET) in order to manufacture low-cost nanofibers with set, predetermined diameters. Thereby, the value of an industrial by-product is remarkably improved by manufacturing products of diverse applicability. Moreover, the utilization of a biowaste material on one hand and a recycled plastic on the other hand has a very positive impact on current environmental issues.

In this article, we report the successful fabrication of nano-sized lignin/recycled PET fibers for the first time via the use of electrospinning. The design of experiments (DoE) statistical methodology was employed in order to optimize the process. Therefore, a road map for the customized fabrication of blended lignin/PET electrospun fibers in the nanometer-scale is presented.

Materials and Methods

Materials

Kraft lignin (low sulfonate content, Mw 10,000 g/mol)was purchased from Sigma-Aldrich and was used without further modification. Waste water-bottles were used as the source of PET. All of them came from the same bottling company in the U.A.E. Prior to the preparation of the spinnable solutions, the bottles were left to dry and then, they were cut into pieces. The Melt Flow Index (MFI) of the used PET was measured to be 72 g/10 min at 265 °C with 2.16 kg load (measurement with a Chengde Jingmi (XRL-400) plastometer according to ASTM D1238). Similar MFI values for PET which has undergone thermal processing cycles, as it is expected for the raw PET used in this research, have been reported elsewhere [27, 28]. For pristine PET, an indicative MFI value found in the literature is 23 g/10 min [28, 29]. For comparison, PET with MFI 20 g/10 min has an indicative molecular weight (M_w) of 42,100 g/mol [30]. Trifluoroacetic acid (TFA, 99 %) purchased from Merck was used as the solvent for the electrospinning process. The solutions of lignin/recycled PET were prepared and left under magnetic stirring at room temperature for 6 h until homogeneously dissolved.

Electrospinning and Experimental Design

The research at this stage involved two steps. The first step was to construct a screening factorial design in a wide experimental area in order to estimate which electrospinning factors influence the average fiber diameter and how. The second step was to estimate the best combination of factors that minimize the average diameter.

The electrospun mats were fabricated in a FUENCE E-sprayer (ES-2000S) apparatus in which the setup has vertical orientation similar to the one shown in Fig. 1. A 10 mL syringe (21G needle) was used. The grounded collector was moving horizontally during the process in a controlled pattern. The design factors of the electrospinning process were the distance between the needle and the collector, the applied voltage, the flow rate of the solution, the concentration of both polymers in the solution and the lignin mass ratio in the polymer blend. Two response variables were chosen; the average fiber diameter and the standard deviation of the fiber diameter.

The levels of the various factors were determined after some preliminary experiments, in which the limits of the experimental area were investigated. For reliably assessing the effect of each factor on the response, it is necessary that the experimental area is as wide as possible, so the range of each factor should be as wide as possible. The criterion for deciding on the range of each factor was the continuous formation of fibers, without spray falling on the collector. In addition, the electrospinning apparatus used in this research has certain limits regarding the allowed values of each factor; the maximum voltage allowed is 30 kV, the maximum spinning distance 20 cm and the minimum flow rate 0.1 μL/min. Therefore, the design factors and their value range, as it was decided after some preliminary experiments, are presented in Table 1. In the electrospinning apparatus used, the fiber spinning was taking place in a closed chamber with controlled ventilation; therefore, all the electrospinning experiments were conducted at room temperature (23 °C) and almost constant humidity (44–46 %).

Factorial designs are the standard methods of experimental design for screening purposes. Screening is an experimental methodology followed when many factors are involved in a process, and it is necessary to examine which of these factors actually influence the response and which don't. In order to avoid an excessive number of experimental runs, it is better to keep the number of factor levels low. Usually two factor levels are enough to characterize the process, and therefore, for each factor only the highest and the lowest value were chosen in order to construct a 2^k factorial design (where k is the number of factors). If more than two levels are chosen for each factor, the number of experiments increases exponentially; if five factors are to be examined, then a two-level full factorial design demands $2^5 = 32$ experimental runs, while a 3-level full factorial design demands $3^5 = 125$ experimental runs. Since a 2-level factorial design can reliable indicate which factors are significant and which are not, it is the best option when many possible factors are involved. More details about the 2^k factorial designs can be found in Ref. [31].

For 5 factors, a 2^5 full factorial design demands 32 unreplicated experimental runs. In order to minimize the experimental runs, only the half fraction of the design was chosen. Therefore a 2^{5-1}, resolution V, fractional factorial design with 16 unreplicated randomized runs was constructed. When only a fraction of the factorial design is run, some information must be sacrificed. This information is the effect of the high-order interactions between the factors. The resolution is an indication of which factor interactions are sacrificed in order to obtain the maximum information under the specific conditions. Particularly, resolution V means that the main factors are aliased with the 4-way interactions and the 2-way interactions are aliased with the 3-way interactions. It is not possible to distinguish the different influence of two aliased effects on the response. However, the high-order interactions (e.g. 3-way, 4-way, etc.) are assumed negligible in most cases.

Table 1 Design factors and their respective levels

Factors	Levels	
	Low	High
Needle-collector distance (*factor A*)	7 cm	20 cm
Concentration of both polymers in the solution (*factor B*)	15 % w/v*	25 % w/v*
Lignin mass ratio in the polymer blend (*factor C*)	20 %	50 %
Voltage (*factor D*)	20 kV	30 kV
Flow rate (*factor E*)	0.1 μL/min	2 μL/min

* The unit w/v denotes weight of polymer (g) per 100 mL volume of solvent

The experiments were conducted by two members of our team. For estimating the possible influence of each operator on the responses, the runs were divided in two blocks. Moreover, two center points were added in each block, in order to add degrees of freedom to the process and estimate the errors more accurately; so, in total, 20 experimental runs were conducted. The experimental design was constructed and analyzed using the Minitab 17 software with 95 % confidence interval(alpha value is 0.05). Figure 2 shows the experimental region and the experimental runs.

Characterization

After the fabrication, all the electrospun samples were left to dry for 24 h at room temperature. The morphology of the fibrous mats was examined via Scanning Electron Microscopy (SEM) (JEOL Neoscope JCM-5000) after gold coating them. The average fiber diameter was measured using an image analyzer (ImageJ, National Institutes of Health, U.S.A.). Around 100 measurements in each sample were used for the calculation of the fiber diameter and the standard deviation. Measurements at several different spots of each SEM image were taken in order to ensure a representative average fiber diameter for each different sample (mat).

Results and Discussion

Electrospinning of Lignin/PET Blend

Figure 3 shows SEM images of various representative electrospun lignin/PET fiber morphologies. The Kraft

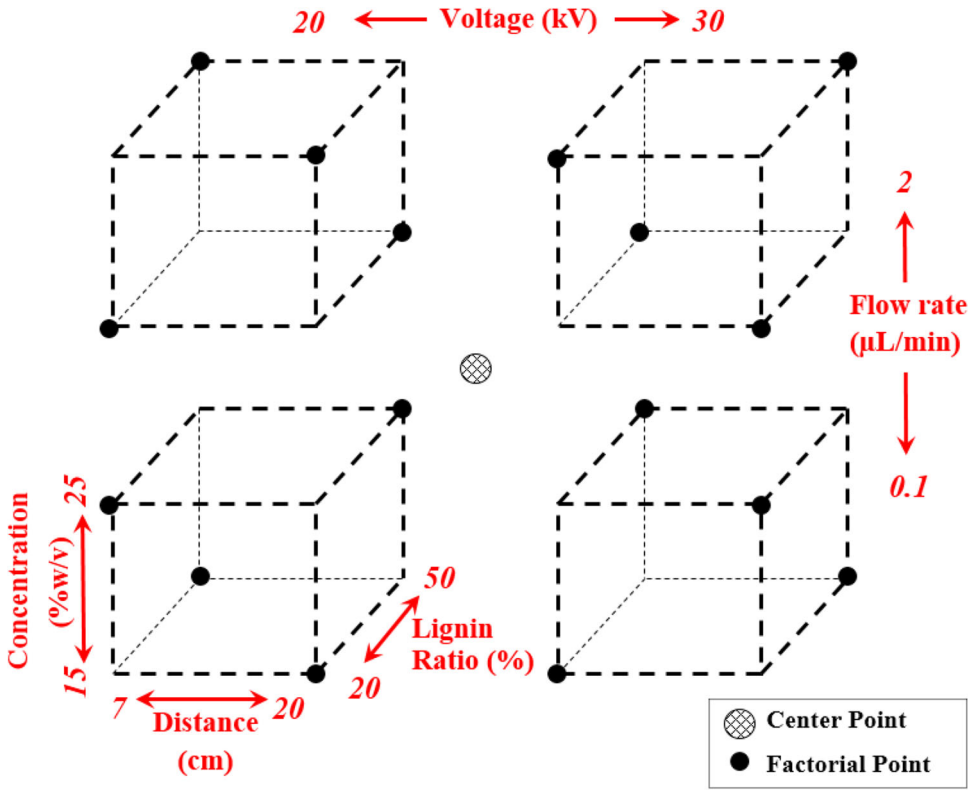

Fig. 2 The 5-dimensional experimental space. Each *dot* represents an experimental run (the center point in the middle of the space is also included)

lignin used in our experiments has a relatively low molecular weight and could only be electrosprayed successfully. Similar behavior has been reported for various types of lignin [25, 26]. Low molecular weight means shorter chains, less polymer entanglements and lower solution viscosity [11, 32]. The solution viscosity is known to influence the morphology and diameter of electrospun fibers; low solution viscosity has been reported to lead to beaded morphology and spray, since the electrospinning jet breaks easily into droplets before falling on the collector [11]. The presence of PET, which plays the role of a binder polymer, was here necessary for the successful fiber fabrication.

The measured average fiber diameter and standard deviation for each experimental run are presented in Table 2.

Average Fiber Diameter: Statistical Analysis of the Factorial Design

For the average diameter, the initial analysis of variance gave the results presented in the Pareto chart of Fig. 4a.

This chart presents the magnitude and relative importance of the standardized effects by displaying their absolute value. Effects lying beyond the reference line are statistically significant. The plot reveals that the only main factors that influence the fiber diameter are the concentration of the solution and the distance between the needle tip and the collector (factors B and A respectively). The lignin ratio, the voltage and the flow rate were found insignificant to the response. Generally, these factors are known to influence the morphology of electrospun fibers [11]. In our case, had we examined an even wider range of values, it is possible that some additional factors would also be significant. However, this specific range of values was based on the demand of acceptable spinnability and was also limited by the apparatus' allowable limits in voltage and spinning distance. In the case of lignin mass ratio, there were spinnability issues at very high percentages of lignin.

Therefore, it was not possible to examine a wider range of these three factors. Even so, all factors influence the response through their interactions. The design was constructed in such way that the 2-way interactions are aliased with the effect of the 3-way interactions. Most probably, however, the high-order effects are a result of the 2-way interactions.

The Pareto chart indicated that the factors BD, AD and CE were not important for the procedure. So, they could be eliminated from the model, together with their aliased ones. Factors C (% lignin), D (voltage) and E (flow rate) couldn't be eliminated, because they participated in significant 2-way interactions. The blocking factor was also found insignificant (p value = 0.785) and it was removed from

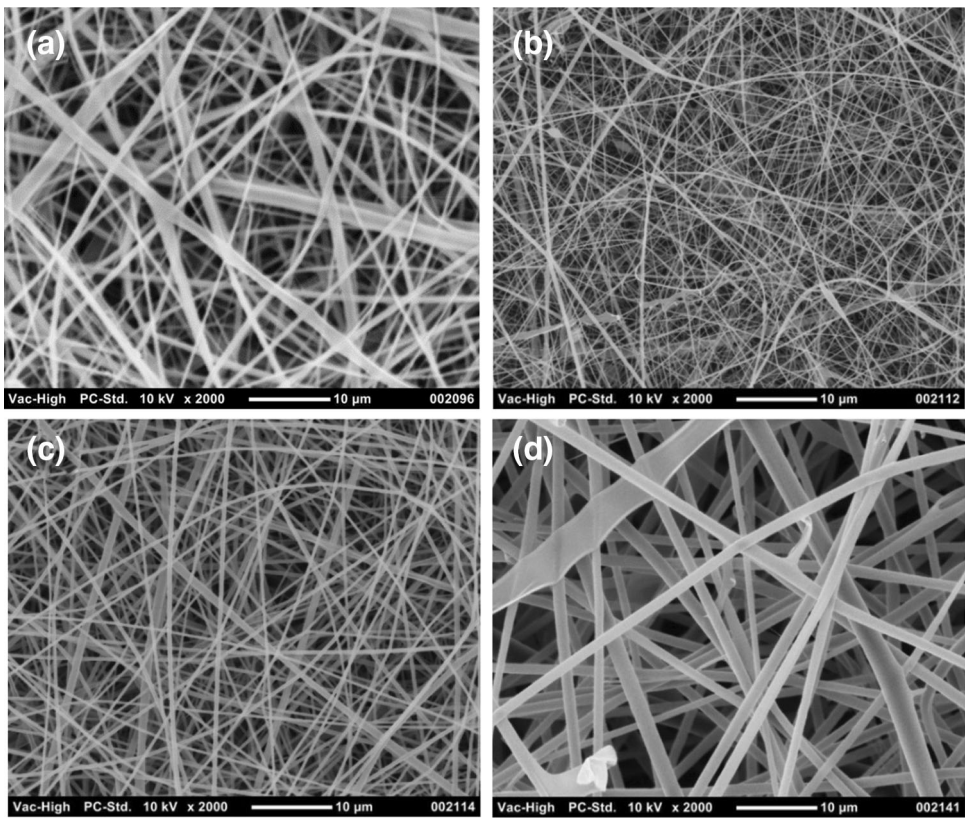

Fig. 3 SEM micrographs of various representative fiber morphologies with varying average diameter;
a 733 ± 388 nm,
b 229 ± 84 nm,
c 462 ± 178 nm,
d 1473 ± 575 nm. *Scale bar* is 10 µm in all images

Table 2 Measured average fiber diameter and standard deviation for each experimental run

Exper. run	Distance (cm)	Concentration (% w/v)	Lignin (%)	Voltage (kV)	Flow rate (μL/min)	Average fiber diameter (nm)	Standard deviation (nm)
1	7.0	25	20	30	2.00	733	388
2	7.0	25	50	30	0.10	455	181
3	20.0	15	50	20	2.00	368	111
4	20.0	15	20	30	2.00	255	68
5	20.0	15	20	20	0.10	325	99
6	13.5	20	35	25	1.05	504	173
7	13.5	20	35	25	1.05	423	246
8	7.0	25	50	20	2.00	670	267
9	20.0	15	50	30	0.10	229	84
10	7.0	25	20	20	0.10	462	178
11	7.0	15	20	30	0.10	328	84
12	7.0	15	20	20	2.00	365	98
13	7.0	15	50	30	2.00	278	71
14	7.0	15	50	20	0.10	278	88
15	13.5	20	35	25	1.05	450	108
16	13.5	20	35	25	1.05	508	168
17	20.0	25	20	20	2.00	639	180
18	20.0	25	20	30	0.10	1145	560
19	20.0	25	50	30	2.00	969	385
20	20.0	25	50	20	0.10	1473	575

the model, as well. This was an indication that the two operators who conducted the experiments did not influence the results.

After elimination of the insignificant factors, the second step of the analysis revealed a similar situation (Fig. 4b). It is important to note here that, now (after the removal of the blocking effect), the AB interaction has a relatively higher effect compared to that in the first step. The reason is that the model was initially designed in such way that the blocking factor was confounded with the AB interaction. Thus, the large AB effect was initially concealed by the very small effect of the blocking factor, and its true effect was revealed after removing the latter.

The actual effect of each factor is concisely presented with its algebraic sign in Table 3. Here, the effects are ranked in a descending order of absolute values. It must be mentioned here, that the actual effect values presented in Table 3 are different from the values shown in the Pareto chart of Fig. 4, because the Pareto chart uses standardized effects based on the t-values of the ANOVA.

The bold solid line in Table 3 indicates the limit below which the effects are insignificant to the response. The variability attributed to the insignificant factors has been eliminated, so now all interactions appear significant. The three main effects C, D and E (lignin mass ratio, voltage and flow rate respectively) still remain insignificant to the response. Interestingly, the product (lignin %) × (voltage) of two insignificant factors appears to have a relatively large effect. It is possible, however, that this significant effect derives from its aliased factor (concentration) × (distance) × (flow rate), where two significant factors participate.

The p value for the model was found 0.000, a strong indication that the model adequately describes the data. A further support to this were the values of R^2 and R^2(pred). R^2 measures the proportion of the total variability explained by the model and in this case it was 99.24 %. The prediction R^2 was found 85.46 %, indicating a model expected to explain around 85 % of the variability in new data. The p-value for the lack-of-fit was 0.307, a proof that the removal of the insignificant factors didn't influence the validity of the model (if the p value of the lack-of-fit was below 0.05 which is the alpha value, it would mean that the model would not be able to describe the data reliably). Finally, the p value for curvature was found 0.019, a sign that in some areas inside the experimental topography, a quadratic model would most accurately fit the data.

The model includes three basic assumptions: that the errors are normally distributed, that they are independently distributed and that their variance is constant. The standardized residual plots of the second step of the analysis (Fig. 5) are useful for testing these assumptions. More

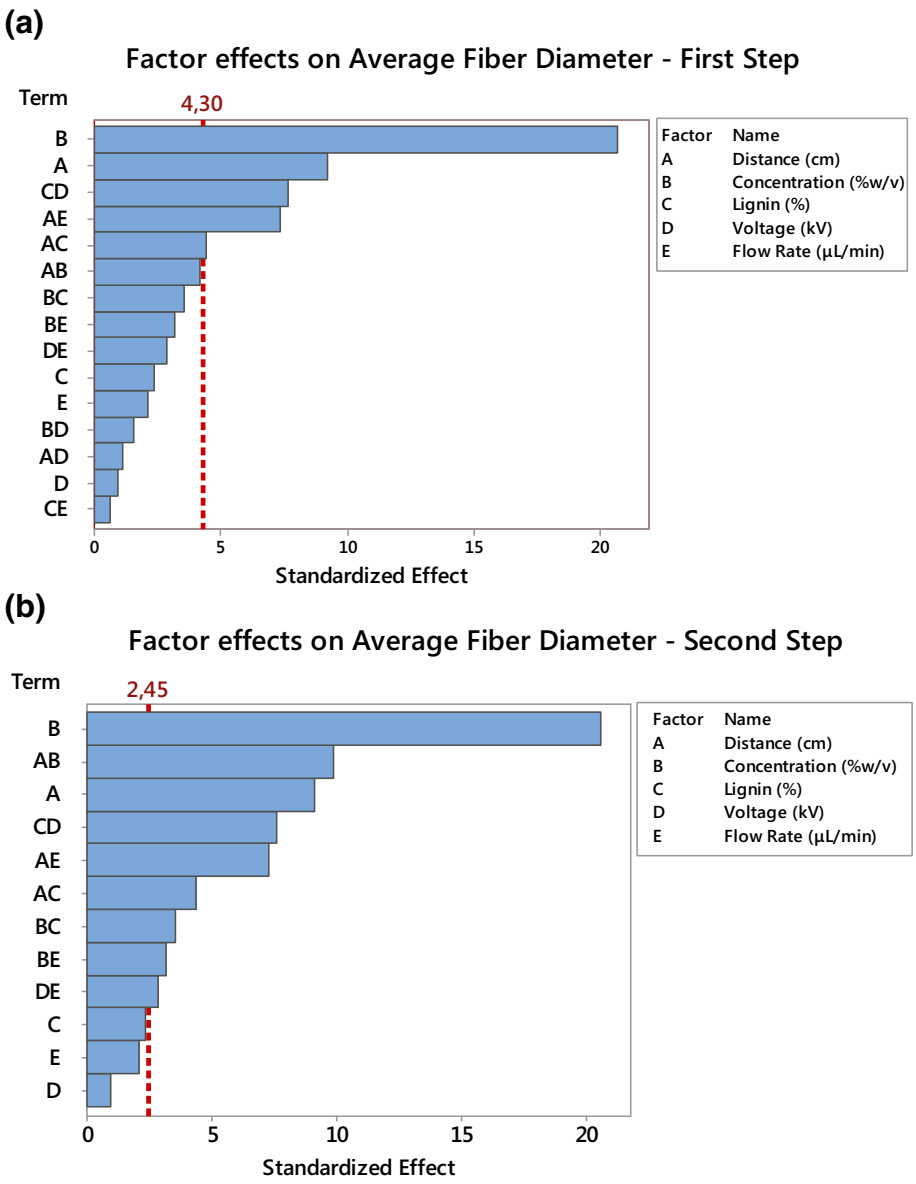

Fig. 4 The standardized effects of electrospinning factors on the average fiber diameter; **a** in the first step of analysis, **b** after eliminating the insignificant interactions

Table 3 Factor effects on average fiber diameter

Factor	Effect
Concentration	+0.5150
(Distance) × (concentration)	+0.2472
Distance	+0.2292
(Lignin %) × (voltage)	−0.1910
(Distance) × (flow rate)	−0.1830
(Distance) × (lignin %)	+0.1103
(Concentration) × (lignin %)	+0.0885
(Concentration) × (flow rate)	−0.0788
(Voltage) × (flow rate)	+0.0718
Lignin %	+0.0585
Flow rate	−0.0523
Voltage	−0.0235

information on the residual plots can be found in Ref. [31]. The normal probability plot confirms that the first assumption is satisfied. Moreover, the plot of the residuals versus observation order follows no obvious pattern, confirming the second assumption.

The plot of standardized residuals versus fitted value is useful for testing the third assumption. This graph shows that all residuals are included in the [−2, 2] range, which is desirable. However, there is much more scatter in the smaller values of response, a sign of higher variability in diameters below 0.5 µm. The explanation for this pattern is that the measurements of fiber diameter through the analysis of SEM images had a higher degree of uncertainty, when measuring narrower fibers. This is rational, because in the SEM images the larger fibers are measured with higher accuracy than the smaller ones. Usually, when

patterns like this appear in the residual plots, a transformation of the response is applied. However, in this case the transformation did not alter the situation. Since we can recognize the source of variability, it is valid to assume that it does not influence the adequacy of the model, especially when all other indicators give acceptable results.

The contour plot of average fiber diameter as a function of the two most significant factors (concentration and spinning distance) is presented in Fig. 6. Here, each shaded area on the plot, corresponds to an experimental region where the fiber diameters have similar values. So, the smallest fiber diameters are found in the darkest areas (diameters <0.4 μm), while the largest diameters appear in the areas of whiter shade (diameters >1.0 μm). The contour plot reveals that the diameter is minimized as the concentration is decreased. However, the contour plot exhibits two areas of minimization (saddle point): in the lowest distance and in the maximum distance. This behavior is reflected in the algebraic values of the effects of concentration, distance and (distance) × (concentration) on the response. It was mentioned earlier that concentration has an effect of +0.5150, distance has an effect of +0.2292 and (distance) × (concentration) has an effect of +0.2472. The two latter effects are very close. The positive sign practically means that an increase in their value tends to increase the diameter. To minimize the response, all three factors [concentration, distance and (distance) × (concentration)] should be set to their lowest values, in order to counteract their positive effect. However, when both distance and concentration are set to their lowest values, then their interaction has its highest value [in coded units this is (−1) × (−1) = (+1)], so it results in increasing the response. When concentration is set to its lowest value and distance to its highest value, their interaction has its lowest value [in coded units (−1) × (+1) = (−1)], but then the adverse effect is caused by the high value of distance. It is not possible to simultaneously minimize all three effects. In each case, a suitable combination of the other factors should be chosen. This behavior guided our next steps towards optimization (see "Minimization of the Average Fiber Diameter" section).

It is well described in the literature that decreasing the concentration of the spinning solution decreases the fiber diameter [11, 17, 33–35]. The reason is that solutions with lower concentration have lower viscosity. As the jet travels towards the collector, the low viscosity facilitates the extension of the jet, resulting in thinner fibers [33].

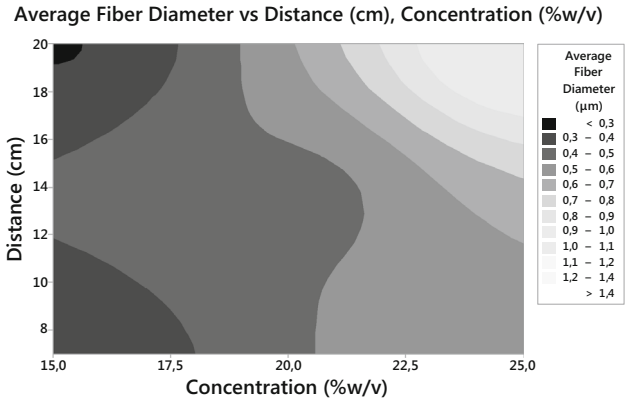

Fig. 6 Contour plot of average fiber diameter versus distance and concentration

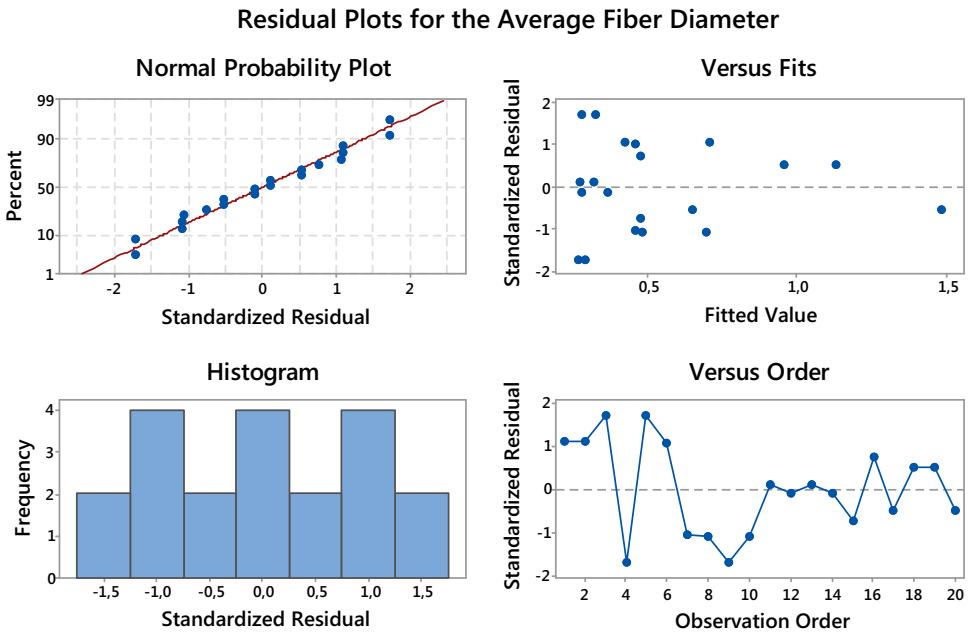

Fig. 5 Standardized residual plots for the average fiber diameter

Theoretically, if the concentration and the viscosity are too low, then the surface tension prevails and the jet breaks up into droplets, resulting in bead formation [33]. The literature gives various possible relationships between the concentration and the fiber diameter (power law, linear, quadratic or cubic relationship) [11, 33].

The effect of spinning distance on fiber diameter is sometimes more complicated. In many cases it has been reported that a larger distance results in thinner fibers [11, 35–37]. When the distance is long enough, the fibers have more time to stretch and elongate under the electrostatic forces before they reach the collector [11, 37]. The solvent evaporation is facilitated and the charged fluid has more time to split into smaller portions [35, 38]. However, different observations have been reported for various systems and there seems to be a more complex relationship [38–41]. In some systems, the increase of distance initially decreases the fiber diameter, but gradually the diameter increases again [39–41]. In these cases, the results are explained by focusing on the strength of the electric field, which is the ratio of voltage over spinning distance [38–41]. At constant voltage, the field is stronger when the distance is small, and gradually weakens with increasing distance. At small spinning distance, the field exerts higher electrostatic force on the jet leading to the formation of thinner fibers [38]. At the same time, a strong field causes higher mass flow, tending to increase the fiber diameter [38]. These antagonistic effects can result in a complex relationship similar to the one observed in our case.

Standard Deviation: Statistical Analysis of the Factorial Design

The selection of the standard deviation of fiber diameter as the second response serves the purpose of investigating in which electrospinning conditions there is a narrower distribution of diameters. The measured standard deviation for each experimental run is presented in Table 2. The analysis of variance revealed which experimental conditions induce higher degree of diameter variation. After eliminating the insignificant factors, the final results are presented in Fig. 7. This plot reveals a situation similar to the average fiber diameter. The only main factors having significant influence on the standard deviation are the concentration and spinning distance (factors B and A respectively), while the other three factors are important only through their interactions. The algebraic signs of the important effects (B, AE, CD, A and AB) were found to be the same as in the case of the average fiber diameter. The p values of the model (0.001) and the lack-of-fit (0.938) and, in addition, the values of R^2 (97.65 %) and R^2 (pred) (88.71 %) confirm the validity of the model.

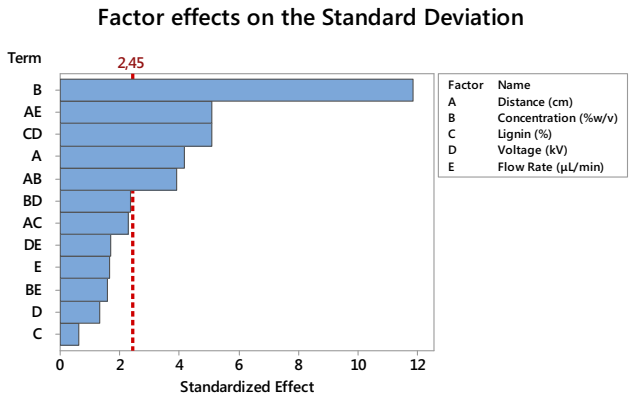

Fig. 7 The standardized factor effects on the standard deviation of fiber diameter

The contour plot of standard deviation versus concentration and distance follows the same pattern with the average fiber diameter (Fig. 8), revealing that the two responses have similar behavior.

The lowest values appear in low levels of concentration, in either the highest or the lowest levels of distance. This seems rational, because when the average diameter has a certain value, the range of similar diameters must be of the same magnitude; for instance, when the average diameter is 1473 nm the standard deviation is 575 nm, while for average diameter of 255 nm the standard deviation is 68 nm. Therefore, in order to estimate more thoroughly in which conditions the narrowest distribution appears, it was more appropriate to use the relative standard deviation, RSD (or coefficient of variation), which is the standard deviation expressed as a percentage of the average fiber diameter. This measure has been used in the literature [38, 42] to estimate the width of the diameter distribution regardless of the diameter magnitude. The RSD for each experimental run is presented in Table 4.

Analysis of variance was performed again considering the RSD as a response and the results are presented in Fig. 9. The results reveal a totally different situation; none of the controllable factors has a significant effect on RSD. The variability of the RSD seems to be a random phenomenon, or at least not depending on the factors examined here. Therefore, it was concluded that the fibrous mats exhibit diameter distribution of similar order of magnitude, regardless of the specific electrospinning conditions.

Minimization of the Average Fiber Diameter

The contour plot in Fig. 6 shows two distinct areas where the fiber diameter decreases (the darkest areas in Fig. 6). The shape of these areas and their position on the graph, next to the plot axes, indicates that they are extended beyond the plot borders, in a wider range of values of concentration and distance. The shape of these areas,

indicates that probably the minimum point lies beyond the plot borders, in values of concentration and distance which were not initially examined. So, it was obvious that it was necessary to explore these areas by examining the values of concentration and distance which would allow the expansion of the experimental region, in order to find the point where the diameter is at its minimum. For achieving this, the method of the steepest descent was followed. This method allows the movement with a specific step towards the direction where the response is most rapidly minimized. Details on this method can be found in Ref. [43].

Figure 10 outlines the paths that allowed the exploration of the areas of interest. The two arrows show the directions, towards which our next experiments progressed; the experiments focused on two distinct areas, Area (1) and Area (2). In Area (1), the concentration and distance were the independent variables, while the other electrospinning factors were held constant. The steepest descent method dictates the progression with a specific step, starting from the center point of the experimental area (in our case concentration 20 % w/v and distance 13.5 cm). According to the method, the step is determined by the variable which has the most significant influence on the response (in our case the concentration) and is equal to the distance between the center point and the factorial points. Applying the principles of the method [43] the necessary step was calculated to be 5 % w/v for the concentration and 2.9 cm for the distance. Four steps were enough to explore this area (Table 5). For practical reasons, the 4th step was not specified by the predetermined step, because it would be irrational to use 0 % w/v concentration. Instead, we decided to use 2.5 %. Based on their interaction effects on the response, and also on the demand of acceptable spinnability in each case, the other variables were held constant at the values which minimized the diameter; that is, voltage = 30 kV, lignin ratio = 50 % and flow rate = 0.1 μL/min.

The maximum allowed distance by the electrospinning apparatus was 20 cm, therefore in Area (2) the only independent variable should be the concentration, since it was not feasible to explore larger values of distance. In this case, however, we decided to use the lignin ratio as a second independent variable. There were indications that an increase in the lignin ratio could give finer fibers,

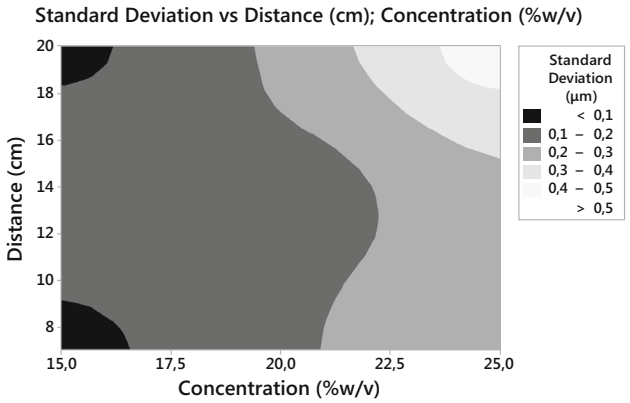

Fig. 8 Contour plot of standard deviation versus concentration and spinning distance

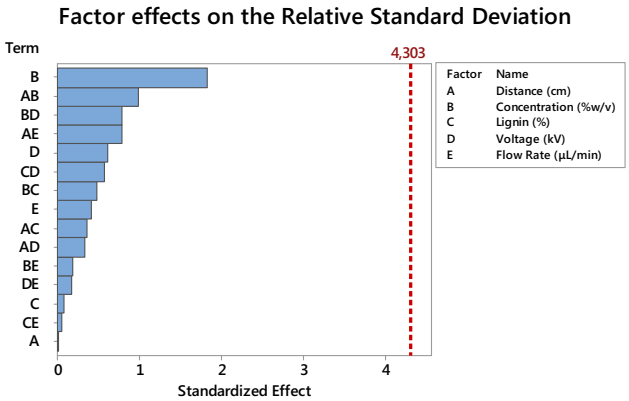

Fig. 9 Effect of the electrospinning factors on relative standard deviation

Table 4 Relative standard deviation (RSD %) for each experimental run

Run order	Average fiber diameter (nm)	RSD %	Run order	Average fiber diameter (nm)	RSD %
1	733	52.9	11	328	25.6
2	455	39.8	12	365	26.8
3	368	30.2	13	278	25.5
4	255	26.7	14	278	31.6
5	325	30.4	15	450	24.0
6	504	34.3	16	508	33.1
7	423	58.1	17	630	28.2
8	670	39.8	18	1145	48.9
9	229	36.7	19	969	39.7
10	462	38.5	20	1473	39.0

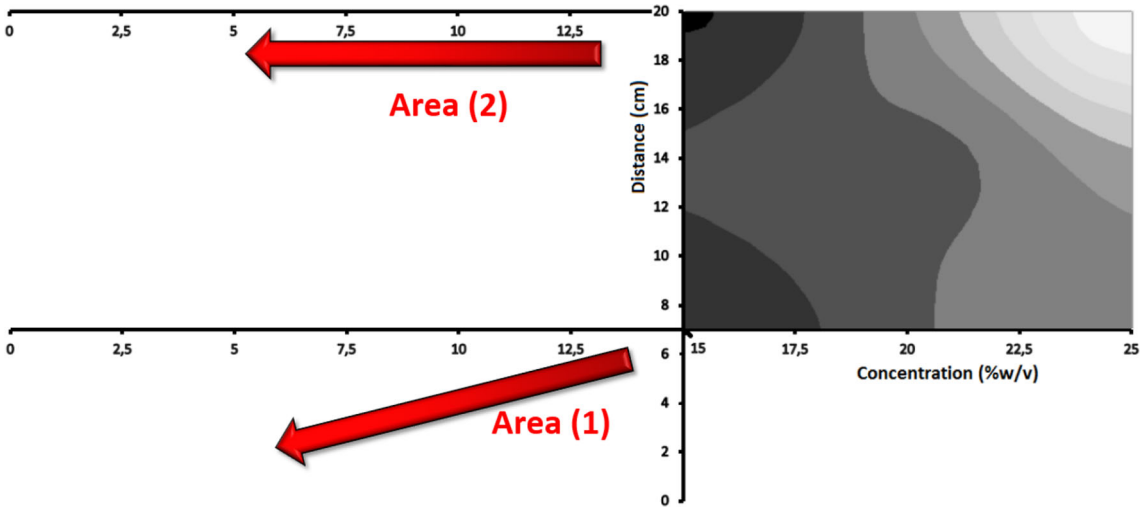

Fig. 10 Experimental paths for the minimization of the average fiber diameter

Table 5 Experimental routes in areas (1) and (2)

Area (1)			Area (2)		
Step	Concentration (% w/v)	Distance (cm)	Step	Concentration (% w/v)	Lignin (%)
1	15	10.6	1	15	50
2	10	7.7	2	11	60
3	5	4.8	3	7	70
4	2.5	1.9	4	4	80
			5	2	90

Table 6 Minimization of the average fiber diameter

Area (1)			Area (2)		
Step	Average diameter (nm)	Standard deviation (nm)	Step	Average diameter (nm)	Standard deviation (nm)
1	250	46	1	234	86
2	191	60	2	211	67
3	183 (*with beads*)	52	3	277 (*with beads*)	63
4	Many beads	–	4	Many beads	–
			5	Only beads	–

although the effect was not very large and too much lignin would have adverse effects in the electrospinnability. Moreover, we decided not to follow strictly the step of the steepest descent method, but to use a slightly smaller one for exploring the area. Based on their interaction effects as well as the demand of acceptable spinnability, the other variables (voltage and flow rate) were held constant at the same values as in the case of Area (1). Briefly, the experimental steps in both areas are summarized in Table 5.

The experimental results in each area are displayed schematically in Fig. 11 and are summarized in Table 6.

In Fig. 11, each experimental run in each of the two areas is denoted with a large dot [four dots in Area (1) and five dots in Area (2)]. For each one of the experimental runs, the SEM image is presented, which shows the morphology of the corresponding electrospun mat. The scale bar in each image is 20 μm. It can be seen, that in some experimental conditions only fibers were produced, and in some others only beaded morphologies.

In both areas the results were similar; starting from step 1 in both areas and moving step-by-step, finer fibers gradually were forming, but at the same time beads progressively appeared until they totally prevailed.

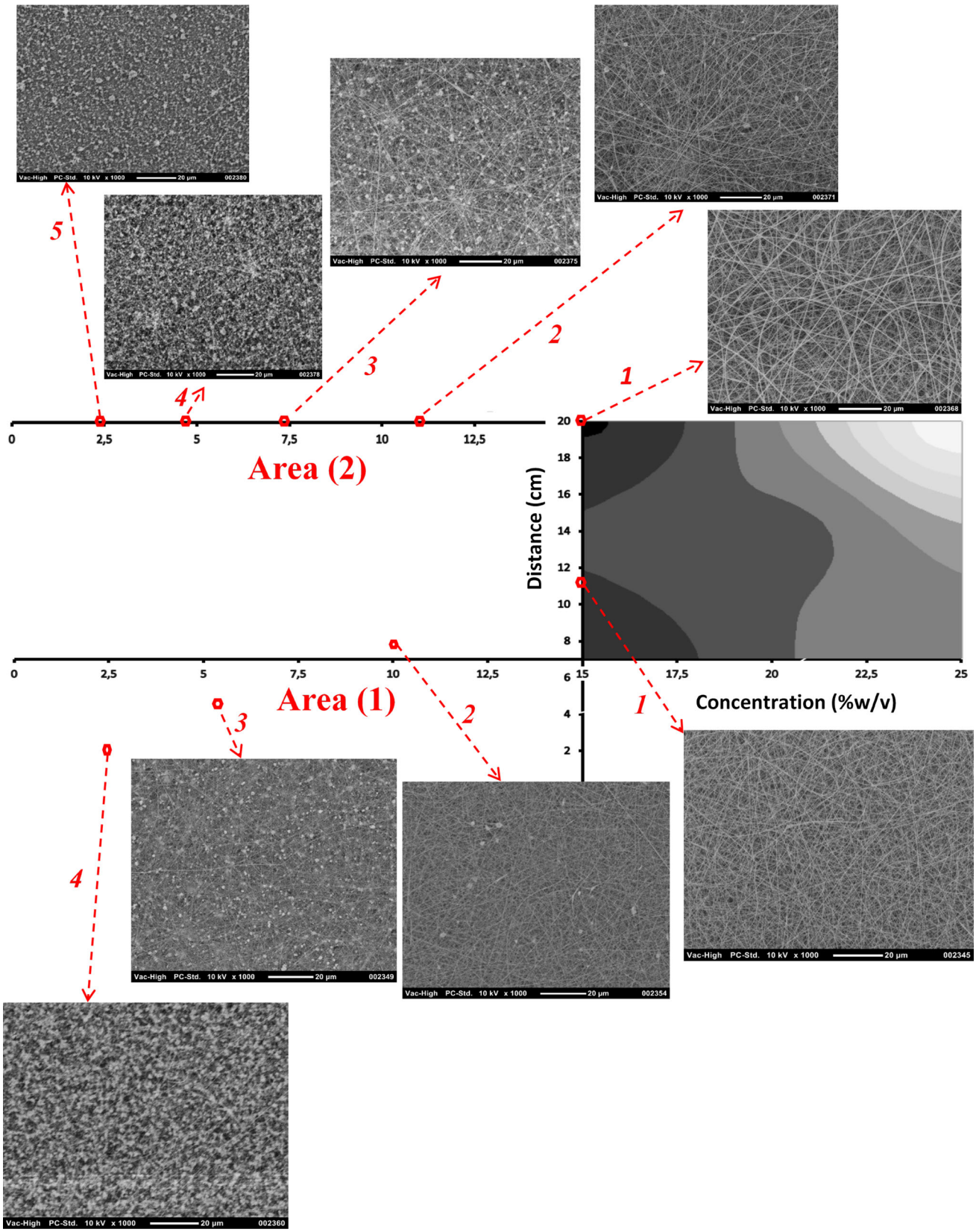

Fig. 11 The results of the steepest descent method. The SEM micrographs have ×1000 magnification

Table 7 Conditions for minimum fiber diameter

Factor	Value
Concentration (%w/v)	10
Lignin ratio (%)	50
Flow rate (μL/min)	0.1
Voltage (kV)	30
Distance (cm)	7.7

Particularly, there was a considerable amount of beads in the third step in both areas, while in the fourth and the fifth step the mat consisted mainly of beads. This was expected and was attributed to the decrease in concentration; similar behavior has been reported for various systems [11, 33]. Lower concentration means lower viscosity [33–35]; thus, the jet broke easily into droplets and beads deposited on the collector. Since it is not desirable to have beads, we decided that the mats beyond the second step were not acceptable in each case. The measurements showed that an average fiber diameter near 200 nm was achieved in both areas, but there were clues that lower average diameter with narrower distribution was achieved in Area (1) (Table 6).

According to the common practice in applying a designed experimental procedure, a Response Surface Methodology should have followed in order to find the exact point of minimization. However, the appearance of beads would make it difficult to accurately define the boundaries of the suitable experimental area. Besides, at such low diameters there is a higher degree of uncertainty in analyzing the SEM images and accurately measuring the exact fiber diameter. So, there was no point in moving a further step with the Response Surface Methodology. Therefore, we concluded that the minimum average fiber diameter (191 nm) is achieved, when the following conditions are applied (Table 7).

Conclusions

A designed experimental approach enabled the reduction of the average diameter of electrospun lignin/recycled PET fibers at the value of 191 ± 60 nm. In the electrospinning process, only the solution concentration and the spinning distance were found to influence the fiber diameter. In contrast, the applied voltage, the flow rate and the lignin ratio in the polymer blend were found insignificant to the fiber diameter and its standard deviation for the range of the experimental factor values examined. None of the electrospinning factors influenced the relative standard deviation of the fiber diameter. By properly reducing the solution concentration and the spinning distance, the average fiber diameter of the electrospun mats was minimized to 191 ± 60 nm. This value represents a scaling down of lignin/PET fiber diameters by two orders of magnitude compared to the diameters of lignin/PET fibers produced by other methods reported in the literature. Minimization of the average fiber diameter at such levels is expected to maximize the surface area of the mats. In potential applications such as substrates for catalysis or adsorption, separators, filters or carbon fiber precursors, maximization of the surface area is of very high importance. The method presented here provides a road map for the fabrication of lignin/PET electrospun mats with nanoscale on-demand diameters by appropriately regulating the electrospinning variables.

Compliance with Ethical Standards

Conflict of interest The authors declare that they have no conflict of interest.

References

1. Thakur VK, Thakur MK, Raghavan P, Kessler MR (2014) ACS Sustain Chem Eng 2:1072–1092. doi:10.1021/sc500087z
2. Alekhina M, Erdmann J, Ebert A et al (2015) J Mater Sci 50:6395–6406. doi:10.1007/s10853-015-9192-9
3. Kim S, Park J, Lee J et al (2015) Fibers Polym 16:744–751. doi:10.1007/s12221-015-0744-z
4. Duval A, Lawoko M (2014) React Funct Polym 85:78–96. doi:10.1016/j.reactfunctpolym.2014.09.017
5. Santos RPO, Rodrigues BVM, Ramires EC et al (2015) Ind Crops Prod 72:1–8. doi:10.1016/j.indcrop.2015.01.024
6. Ruiz-Rosas R, Bedia J, Lallave M et al (2010) Carbon N Y 48:696–705. doi:10.1016/j.carbon.2009.10.014
7. Ragauskas AJ, Beckham GT, Biddy MJ et al (2014) Science 344:1246843. doi:10.1126/science.1246843
8. Frank E, Steudle LM, Ingildeev D et al (2014) Angew Chemie Int Ed 53:5262–5298. doi:10.1002/anie.201306129
9. Wang C-Q, Wang H, Liu Y-N (2015) Waste Manag 35:42–47. doi:10.1016/j.wasman.2014.09.025
10. NAPCOR—National Association for PET Container Resources (USA). http://www.napcor.com/PET/landing_petrecycling.html. Accessed 31 May 2016
11. Ko F, Wan Y (2014) Introduction to nanofiber materials. Cambridge University Press, Cambridge, pp 49–58
12. Hao J, Lei G, Li Z et al (2013) J Memb Sci 428:11–16. doi:10.1016/j.memsci.2012.09.058
13. Chen C, Wang L, Huang Y (2008) Mater Lett 62:3515–3517. doi:10.1016/j.matlet.2008.03.034
14. Meng X, Luo N, Cao S et al (2009) Mater Lett 63:1401–1403. doi:10.1016/j.matlet.2009.03.023
15. Chen C, Wang L, Huang Y (2008) Sol Energy Mater Sol Cells 92:1382–1387. doi:10.1016/j.solmat.2008.05.013
16. Hoover LA, Schiffman JD, Elimelech M (2013) Desalination 308:73–81. doi:10.1016/j.desal.2012.07.019
17. Hadjizadeh A, Ajji A, Bureau MN (2011) J Mech Behav Biomed Mater 4:340–351. doi:10.1016/j.jmbbm.2010.10.014
18. Persano L, Camposeo A, Pisignano D (2014) Prog Polym Sci 43:48–95. doi:10.1016/j.progpolymsci.2014.10.001

19. Kadla JF, Kubo S, Gilbert RD, Venditti RA (2002) Lignin-based carbon fibers. In: Hu TQ (ed) Chemical modification, properties and usage of lignin. Kluwer Academic, Berlin, pp 121–137
20. Kubo S, Kadla JF (2005) J Polym Environ 13:97–105. doi:10.1007/s10924-005-2941-0
21. Compere AL, Griffith WL, Leitten CF, Pickel JM (2005) Evaluation of lignin from alkaline-pulped hardwood black liquor, Oak Ridge National Laboratory, May 2005. http://web.ornl.gov/info/reports/2005/3445605475900.pdf
22. Kadla JF, Kubo S (2004) Compos A Appl Sci Manuf 35:395–400. doi:10.1016/j.compositesa.2003.09.019
23. Canetti M, Bertini F (2007) Compos Sci Technol 67:3151–3157. doi:10.1016/j.compscitech.2007.04.013
24. Canetti M, Bertini F (2009) E-Polymers. doi: 10.1016/S0032
25. Dallmeyer I, Ko F, Kadla JF (2010) J Wood Chem Technol 30:315–329. doi:10.1080/02773813.2010.527782
26. Choi DI, Lee J-N, Song J et al (2013) J Solid State Electrochem 17:2471–2475. doi:10.1007/s10008-013-2112-5
27. Srithep Y, Javadi A, Pilla S et al (2011) Polym Eng Sci 51:1023. doi:10.1002/pen
28. Spinace MAS, De Paoli MA (2001) J Appl Polym Sci 80:20–25
29. Pesetskii SS, Jurkowski B, Filimonov OV et al (2010) J Appl Polym Sci 119:225–234
30. Khoffi F, Khenoussi N, Harzallah O, Drean J (2011) Phys Procedia 21:240–245. doi:10.1016/j.phpro.2011.11.001
31. Montgomery DC (2013) Design and Analysis of Experiments. Wiley, 8th ed, international student version, chapters 5–8
32. Brazen CS, Rosen SL (2012) Fundamental Principles of Polymeric Materials. Wiley, 3rd ed. chapter 14
33. Gu SY, Ren J, Vancso GJ (2005) Eur Polym J 41:2559–2568. doi:10.1016/j.eurpolymj.2005.05.008
34. Dallmeyer I, Ko F, Kadla JF (2014) Ind Eng Chem Res 53:2697–2705. doi:10.1021/ie403724y
35. Li Y, Huang Z, Lǔ Y (2006) Eur Polym J 42:1696–1704. doi:10.1016/j.eurpolymj.2006.02.002
36. Thompson CJ, Chase GG, Yarin AL, Reneker DH (2007) Polymer (Guildf) 48:6913–6922. doi:10.1016/j.polymer.2007.09.017
37. Awal A, Sain M, Chowdhury M (2011) Compos B Eng 42:1220–1225. doi:10.1016/j.compositesb.2011.02.011
38. Heikkilä P, Harlin A (2008) Eur Polym J 44:3067–3079. doi:10.1016/j.eurpolymj.2008.06.032
39. Park JY, Lee IH, Bea GN (2008) J Ind Eng Chem 14:707–713. doi:10.1016/j.jiec.2008.03.006
40. Cramariuc B, Cramariuc R, Scarlet R et al (2013) J Electrostat 71:189–198. doi:10.1016/j.elstat.2012.12.018
41. Kong L, Ziegler GR (2013) Carbohydr Polym 92:1416–1422. doi:10.1016/j.carbpol.2012.09.026
42. Yördem OS, Papila M, Menceloğlu YZ (2008) Mater Des 29:34–44. doi:10.1016/j.matdes.2006.12.013
43. Montgomery DC (2013) Design and analysis of experiments. Wiley, 8th edition/international student version, chapter 11